Cellular/Molecular

Sleep Slow Wave-Related Homo and Heterosynaptic LTD of Intrathalamic $GABA_A$ergic Synapses: Involvement of T-Type Ca^{2+} Channels and Metabotropic Glutamate Receptors

Romain Pigeat,[1,2,3] Patrick Chausson,[1,2,3] Fanny M. Dreyfus,[1,2,3] Nathalie Leresche,[1,2,3]* and Régis C. Lambert[1,2,3]*

[1]Sorbonne Universités, UPMC University Paris 06, UM 119, Neuroscience Paris Seine (NPS), Paris F-75005, France, [2]CNRS, UMR 8246, NPS, Paris F-75005, France, and [3]INSERM, U1130, NPS, Paris F-75005, France

Slow waves of non-REM sleep are suggested to play a role in shaping synaptic connectivity to consolidate recently acquired memories and/or restore synaptic homeostasis. During sleep slow waves, both GABAergic neurons of the nucleus reticularis thalami (NRT) and thalamocortical (TC) neurons discharge high-frequency bursts of action potentials mediated by low-threshold calcium spikes due to T-type Ca^{2+} channel activation. Although such activity of the intrathalamic network characterized by high-frequency firing and calcium influx is highly suited to modify synaptic efficacy, very little is still known about its consequences on intrathalamic synapse strength. Combining *in vitro* electrophysiological recordings and calcium imaging, here we show that the inhibitory GABAergic synapses between NRT and TC neurons of the rat somatosensory nucleus develop a long-term depression (I-LTD) when challenged by a stimulation paradigm that mimics the thalamic network activity occurring during sleep slow waves. The mechanism underlying this plasticity presents unique features as it is both heterosynaptic and homosynaptic in nature and requires Ca^{2+} entry selectively through T-type Ca^{2+} channels and activation of the Ca^{2+}-activated phosphatase, calcineurin. We propose that during slow-wave sleep the tight functional coupling between $GABA_A$ receptors, calcineurin, and T-type Ca^{2+} channels will elicit LTD of the activated GABAergic synapses when coupled with concomitant activation of metabotropic glutamate receptors postsynaptic to cortical afferences. This I-LTD may be a key element involved in the reshaping of the somatosensory information pathway during sleep.

Key words: **calcineurin; $GABA_A$ receptor; low-threshold calcium spike; nucleus reticularis thalami; synaptic plasticity; ventrobasal thalamic nucleus**

Introduction

Increasing evidence demonstrates that slow waves of non-REM sleep are involved in memory consolidation (Diekelmann and Born, 2010) and may participate in synaptic homeostasis (Tononi and Cirelli, 2014), both processes involving reshaping of synaptic connectivity. At the thalamic level, the two components of sleep slow waves (i.e., slow <1 Hz and delta waves) are characterized by the almost regular occurrence of high-frequency bursts of action potentials mediated by low-threshold calcium spikes in its two major and interconnected cell types, i.e., the thalamocortical (TC) neurons and the GABAergic neurons of the nucleus reticularis thalami (NRT; Domich et al., 1986; Steriade et al., 1993). These low-threshold calcium spikes are mediated by T-type Ca^{2+} channel activation which, in both cell types, elicit a large global influx of calcium across the entire dendritic arbor (Crandall et al., 2010; Errington et al., 2010; Chausson et al., 2013). As a consequence, a tight association between a presynaptic neuron displaying high-frequency firing and a postsynaptic neuron showing a large concomitant Ca^{2+} influx characterizes the activity of the intrathalamic network during slow waves of non-REM sleep. Surprisingly, although (1) many experiments in other neuronal types have shown that similar patterns of discharge coupled to postsynaptic Ca^{2+} entry are highly suited to modify synaptic strength (Citri and Malenka, 2008) and (2) modifications in intrathalamic functional connectivity should drastically impact information transfer to and between cortical areas (Sherman and Guillery, 1996; Castro-Alamancos and Calcagnotto, 1999), selective attention (Crick, 1984; Weese et al., 1999; McAlonan et al., 2006, 2008; Higley and Contreras, 2007), and patho/physiological brain rhythm generation (Steriade et al., 1993; Crunelli and Leresche, 2002; Leresche et al., 2012), very little is still known about the consequences of non-REM sleep activity on thalamic synaptic plasticity.

Here, using a combination of *in vitro* electrophysiological recordings and two-photon calcium imaging in the somatosensory thalamus, we show that a stimulation paradigm that tightly mimics the thalamic network activity occurring during sleep slow waves elicits a long-term depression (I-LDT) at the GABAergic

Received July 4, 2014; revised Oct. 21, 2014; accepted Nov. 5, 2014.

Author contributions: N.L. and R.C.L. designed research; R.P., P.C., F.M.D., N.L., and R.C.L. performed research; R.P., P.C., F.M.D., N.L., and R.C.L. analyzed data; R.P., N.L., and R.C.L. wrote the paper.

This work was supported by ANR-MNMP-2009. We thank Dr. E. Guiot for assistance in calcium imaging and Drs. V.N. Uebele and J.J. Renger from Merck and Co. (USA) for their kind gift of TTA-P2.

*N.L. and R.C.L. contributed equally to the work.

The authors declare no competing financial interests.

Correspondence should be addressed to Régis C. Lambert, Neuroscience Paris Seine (NPS), Université Pierre et Marie Curie, 9 quai St. Bernard, Paris F-75005 France. E-mail: regis.lambert@upmc.fr.

DOI:10.1523/JNEUROSCI.2748-14.2015

 0270-6474/15/350064-10$15.00/0

synapse between NRT and TC neurons of the ventrobasal nucleus (VB). The mechanism underlying this synaptic plasticity presents unique features, as it depends on activation of type 1 mGluRs, $GABA_A$ receptors, and an influx of Ca^{2+} selectively through T-type channels, which, in turn, triggers the activation of the Ca^{2+}/calmodulin-dependent phosphatase 2B, calcineurin. Therefore, we propose that a tight functional coupling exists between $GABA_A$ receptors, calcineurin, and T-type Ca^{2+} channels at the NRT-TC inhibitory synapses, which during slow-wave sleep allows expression of LTD of the activated GABAergic synapses.

Materials and Methods

All procedures involving experimental animals were performed in accordance with the EU Council Directive 86-609 and local ethics committee guidelines. All efforts were made to minimize animal suffering and the number of animals used.

Slice preparation. Brains were excised from 12- to 18-d-old male Wistar rats. A block of tissue containing the thalamus was removed and placed in a cold (<4°C) oxygenated (95% O_2; 5% CO_2) solution of aCSF containing the following (in mM): 125 NaCl, 2.5 KCl, 0.4 $CaCl_2$, 1 $MgCl_2$, 1.25 NaH_2PO_4, 26 $NaHCO_3$, 25 glucose, 5 Na-pyruvate, and 1 kynurenic acid, pH 7.3, osmolarity 310 mOsm. The block of tissue was glued, ventral surface uppermost, to the stage of a vibroslice (Leica VT1000S), and 280–300-μm-thick horizontal slices containing the VB and the NRT were prepared using the internal capsule and the medial lemniscus as landmarks.

Slices (three to four per hemisphere) were stored in an oxygenated incubation chamber containing aCSF of the above composition, but without kynurenic acid and with 2 mM $CaCl_2$, for at least 1 h before being transferred to the recording chamber, where they were perfused (2.5 ml/min) continuously with an oxygenated recording solution of the same composition at room temperature or at 32°C.

Electrophysiology. Using the patch-clamp technique (Axopatch 200B amplifier, Clampex 10; Molecular Devices), whole-cell recordings in voltage-clamp mode were performed in neurons of the VB visualized with an Olympus BX51WI (60× lens). Current recordings were filtered by a four-pole Bessel filter set at a corner frequency of 2 kHz, digitalized at 10 kHz, and later analyzed using Clampfit 10 (Molecular Devices) and Igor 6 (WaveMetrics). Recording electrodes (borosilicate glass capillaries; WPI) were filled with the following (in mM): 128 methanesulfonic acid, 12 CsCl, 10 HEPES, 0.5 EGTA, 0.1 $CaCl_2$, 3 $MgCl_2$, 4 Na-ATP, 0.4 Na-GTP, 15 phosphocreatine, and 150 U/ml creatine phosphokinase, pH 7.3, with CsOH, and osmolarity 280 mOsm (tip resistances: 1.8–2.8 MΩ; access resistance: 2–12 MΩ). The resulting Cl^- inversion potential was −50 mV. In some recordings, 10 mM BAPTA (Sigma-Aldrich) or 2 mg/ml biocytin (Sigma-Aldrich) was included in the pipette. At least 70% of the cell capacitance and series resistance was compensated. The liquid junction potential (+6 mV) was systematically corrected.

IPSCs (150–700 pA) were evoked every 30 s by electric pulses (40–100 μs, 5–20 V) delivered by a monopolar, borosilicate glass stimulating electrode filled with extracellular medium and placed >100 μm away from the soma of the recorded neuron (Fig. 1*A*). Isolation of $GABA_A$ IPSCs was achieved by the addition of 50 μM DL-APV and 10 μM CNQX to the perfusion medium. Membrane resistance (>100 MΩ) was monitored throughout the experiment and data were discarded if >20% change of the membrane resistance was observed.

In some experiments, a second monopolar borosilicate glass electrode was added to stimulate in isolation two bundles of NRT afferences impinging on the recorded TC neuron. To ensure the independence of the two pathways, we assessed the lack of paired-pulse depression of the IPSCs evoked by one stimulating electrode following a preceding (100 ms) stimulation through the other electrode.

For the experiments using calcineurin antagonists, slices were first incubated for 1 h in Cyclosporin A (CyA) and FK-506 (at 25 and 50 μM, respectively) and then perfused with 10 μM CyA and 20 μM FK-506. CyA was dissolved in EtOH:Tween 80 with a final concentration in aCSF of 0.1%:0.05%.

LTD induction protocol. Induction protocols consisted of four bursts of seven stimulations at 200 Hz that were delivered at a frequency of 1.6 Hz through the stimulating electrode. Each burst of synaptic stimulations was paired to a 50 ms depolarization of the TC neuron from −80 mV to various test potentials (between −30 and +10 mV; see Results for details; Fig. 1*A*). Unless otherwise specified, the stimulation train started at the onset of the depolarizing step. The protocol was repeated seven times at 0.14 Hz. Only one induction protocol was delivered per slice. Changes in synaptic efficacy were quantified as the ratio between the mean IPSC amplitudes over 10 min periods calculated before and 20 min after the induction protocol.

Histology. At the end of the recordings, slices containing biocytin-filled neurons were fixed overnight by immersion in 4% paraformaldehyde and then washed with 0.1% PBS. After incubating the slices with 0.4% Triton X-100 and PBS (1 h), biocytin-filled neurons were revealed using Streptavidin Alexa Fluor 488 (1:1000; 2–3 h in dark; Invitrogen). Slices were then washed in PBS Triton 0.4% (1 h) before being immerged in PBS and mounted on cover slides.

Ca^{2+} imaging. For Ca^{2+} imaging, intracellular solution without EGTA was supplemented with the Ca^{2+} indicator Fluo-5F (300 μM; Invitrogen) and Alexa Fluor 594 (15 μM; Invitrogen). Neurons were loaded with indicators for 30 min before acquisition. Two-photon excitation of the fluorescent dyes (custom-built two-photon laser scanning microscope) was performed by a femtosecond Ti:sapphire laser (Mai Tai HP; Spectra-Physics) tuned to 800 nm and fluorescent signals were acquired simultaneously across dendrites at selected regions of interest (acquisition frequency = 40–60 frames/s) by two high-gain photomultiplier tubes (Hamamatsu H9305-03). At the end of the recordings *Z*-series of 160–190 images (512 × 512 pixels, 0.26 μm/pixel) were taken with 0.5 μm focal steps to construct a 2D maximum intensity projection of each neuron. Image acquisition was controlled by MPScope software (Nguyen et al., 2006). The reported change in fluorescence ($\Delta G/R$) was calculated as the change in fluorescence (G_{peak}) from baseline (G_0, average of the 400 ms period before stimulus) of the Ca^{2+}-sensitive indicator (Fluo-5F) normalized to the average fluorescence of the Ca^{2+}-insensitive indicator (R_{Avg}, Alexa Fluor 594): $\Delta G/r = (G_{peak} - G_0)/R_{Avg}$.

Drugs. CNQX, DL-AP5, CGP-55845A, SR95531, and LY-341495 were obtained from Tocris Bioscience, LY-367385 and furosemide from Sigma-Aldrich, Cyclosporin A from Abcam, and FK-506 from AbMole. TTA-P2 (provided by Merck), was made up as 10 mM stock solution in dimethylsulfoxide and kept at −20°C until use.

Statistical analysis. Quantitative data in the text and figures are given as mean ± SEM. Paired Student's *t* test was used to compare the value of average IPSCs and paired-pulse depression before and after the induction protocol. Wilcoxon signed-rank test was used as appropriate to compare the value of $\Delta G/R$.s.

Results

Thalamic slow-wave activity induces LTD of the NRT-TC inhibitory synapse

In TC neurons hold at −80 mV; inward $GABA_A$ergic currents ($E_{Cl} = -50$ mV) were evoked in the continuous presence of the ionotropic glutamate receptor antagonists CNQX (10 μM) and DLAPV (50 μM) by extracellular stimulation of the afferent NRT fibers (Fig. 1*A*). After a stable baseline recording, short series of periodic (1.6 Hz) high-frequency stimulations (200 Hz) were applied to the NRT afferences while depolarizing the postsynaptic TC neurons from −80 to −30 mV at the same time of the presynaptic stimulation. This induction protocol mimics the incoming bursting activity of the NRT fibers and the concomitant low-threshold spike (LTS)-associated depolarization of the TC neurons that occur during sleep slow waves (Fig. 1*A*; see Materials and Methods for details of the protocol). The periodicity of stimulation trains was chosen to be in the low range of the δ rhythmic activities reported in NRT neurons (Amzica et al., 1992; Contreras and Steriade, 1997). As illustrated in Figure 1, *B* and *C*, these physiological-like stimulations induced a clear depression of the inhibitory $GABA_A$ postsynaptic currents (IPSCs) that reached a steady state of 73 ± 2% (compared with baseline; n =

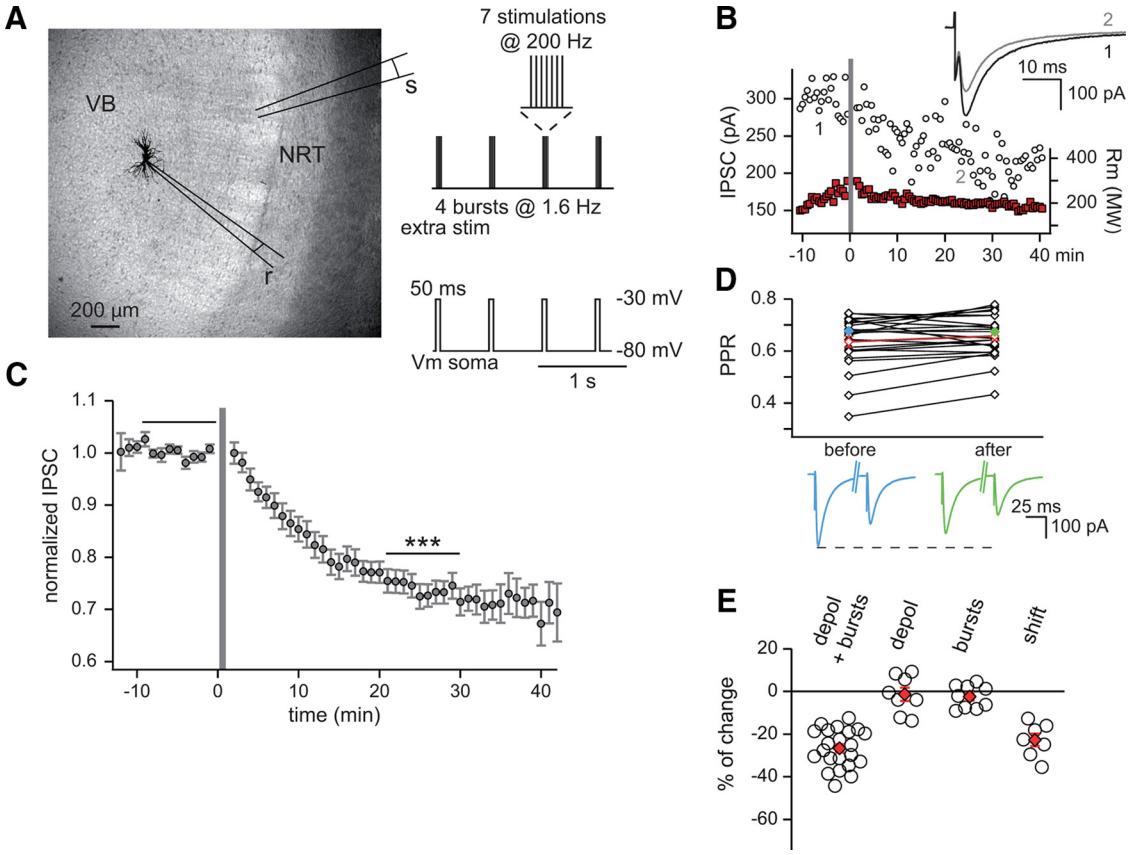

Figure 1. LTD of the GABAergic NRT-TC synapses is induced by sleep slow wave-like activities. ***A***, Bright-field image of a thalamic slice (left) and schematic representation of the induction protocol (right). Extracellular electrode (s) was used to stimulate afferent fibers to the biocytin-stained TC recorded in the VB. Patch pipette, r. Induction protocol consisted of four stimulating bursts delivered at a frequency of 1.6 Hz. Each burst contained seven stimulations at 200 Hz and was paired to a 50 ms depolarization of the TC neuron. This sequence was repeated seven times at 0.14 Hz. ***B***, Amplitude of IPSCs (open circle) and value of input resistance (Rm; red square) plotted against time for a representative neuron. The induction protocol indicated by a gray bar was applied following a 10 min baseline. Averages of 20 IPSCs recorded during baseline (1, black) or 20–30 min after the induction protocol (2, gray) are superimposed above the graph. ***C***, Summary graph of 22 experiments performed as in ***B***. For each neuron the amplitude of the IPSCs was normalized to the mean IPSC amplitude of the baseline period. The magnitude of the I-LTD was quantified by the ratio between the average amplitude of the responses recorded between 20 and 30 min after the induction protocol and during the 10 min preceding the induction protocol (periods indicated by the black bars; $^{***}p < 0.001$). ***D***, Paired-pulse ratio of two consecutive IPSCs 100 ms apart (PPR: second IPSC amplitude/first IPSC amplitude) measured during the baseline period (before) and 20–30 after the induction protocol (after). Black diamonds represent individual experiments ($n = 22$) and the red diamonds symbolize the average value of the PPR. Traces below are examples of 100 ms paired-evoked IPSCs recorded in one of the TC neurons before (blue) and after (green) the induction protocol (the corresponding PPR values are depicted by blue and green diamonds in the graph). Note that the LTD of the IPSCs is not associated with changes in PPR. ***E***, Plot of percentage changes in IPSC amplitude observed 20–30 min after four different induction protocols consisting of (1) the paired protocol illustrated in ***A*** (depol + bursts, $n = 22$), (2) the depolarization of the TC neuron without stimulation of the afferences (depol, $n = 7$), (3) stimulation of the afferents without depolarization of the TC neuron (bursts, $n = 9$), or (4) paired protocol in which stimulations occurred 20 ms after the onset of the TC neuron depolarization (shift, $n = 7$). The red circle indicates the mean value of the changes in IPSC amplitude in each condition.

22, $p < 0.001$) ~20 min after the induction protocol. Similar results were obtained when recording at 32°C (postprotocol IPSC amplitude: 74 ± 5% of baseline, $n = 4$, $p < 0.05$; data not shown). Consistent with a postsynaptic locus of expression of this I-LTD, the paired-pulse depressions evaluated from two consecutive IPSCs 25 ms, 50 ms, or 100 ms apart were unchanged (25 ms: baseline 0.76 ± 0.21, postprotocol 0.80 ± 0.24, $n = 4$; 50 ms: baseline 0.69 ± 0.07, postprotocol 0.73 ± 0.09, $n = 4$; 100 ms: baseline 0.64 ± 0.02, postprotocol 0.66 ± 0.02, $n = 22$, $p > 0.05$; Fig. 1*D*). As the range of paired-pulse ratio values was large, we checked that this ratio evaluated from two consecutive IPSCs 100 ms apart was not correlated to the magnitude of the I-LTD (linear correlation test, $p > 0.1$).

Although the precise timing between NRT neuron-bursting activities and TC neuron LTS generation during sleep slow waves is unknown, the collateral innervation of the NRT by TC fibers suggests that burst firing in NRT neurons should occur a few tens of milliseconds after the beginning of a TC neuron LTS. Therefore, we checked that the I-LTD was readily induced when the train of NRT fiber stimulation occurred 20 ms after the onset of the TC neuron depolarization (postprotocol IPSC amplitude: 77 ± 3% of baseline, $n = 7$, $p < 0.01$; Fig. 1*E*). In contrast, no I-LTDs were observed in experiments where either the NRT fiber stimulations or the TC neuron depolarizations were omitted in the induction protocol (postprotocol IPSC amplitude: 98 ± 2 and 99 ± 3% of baseline, $n = 9$ and 8, respectively, $p > 0.05$; Fig. 1*E*) indicating that both the presynaptic and postsynaptic components of the induction protocol were required to induce the I-LTD.

Selective Ca^{2+} influx through the T-type channels is required for I-LTD induction

As shown in Figure 2*A*, two-photon calcium imaging indicated that repetitive depolarizations from −80 to −30 mV induced a robust increase in intracellular Ca^{2+} concentration throughout the TC neuron dendritic arborization. To investigate the contribution of calcium influx in TC neurons to the I-LTD induction we first added the fast Ca^{2+} chelator, BAPTA (10 mM), in the intrapipette solution. In this recording condition, no depression

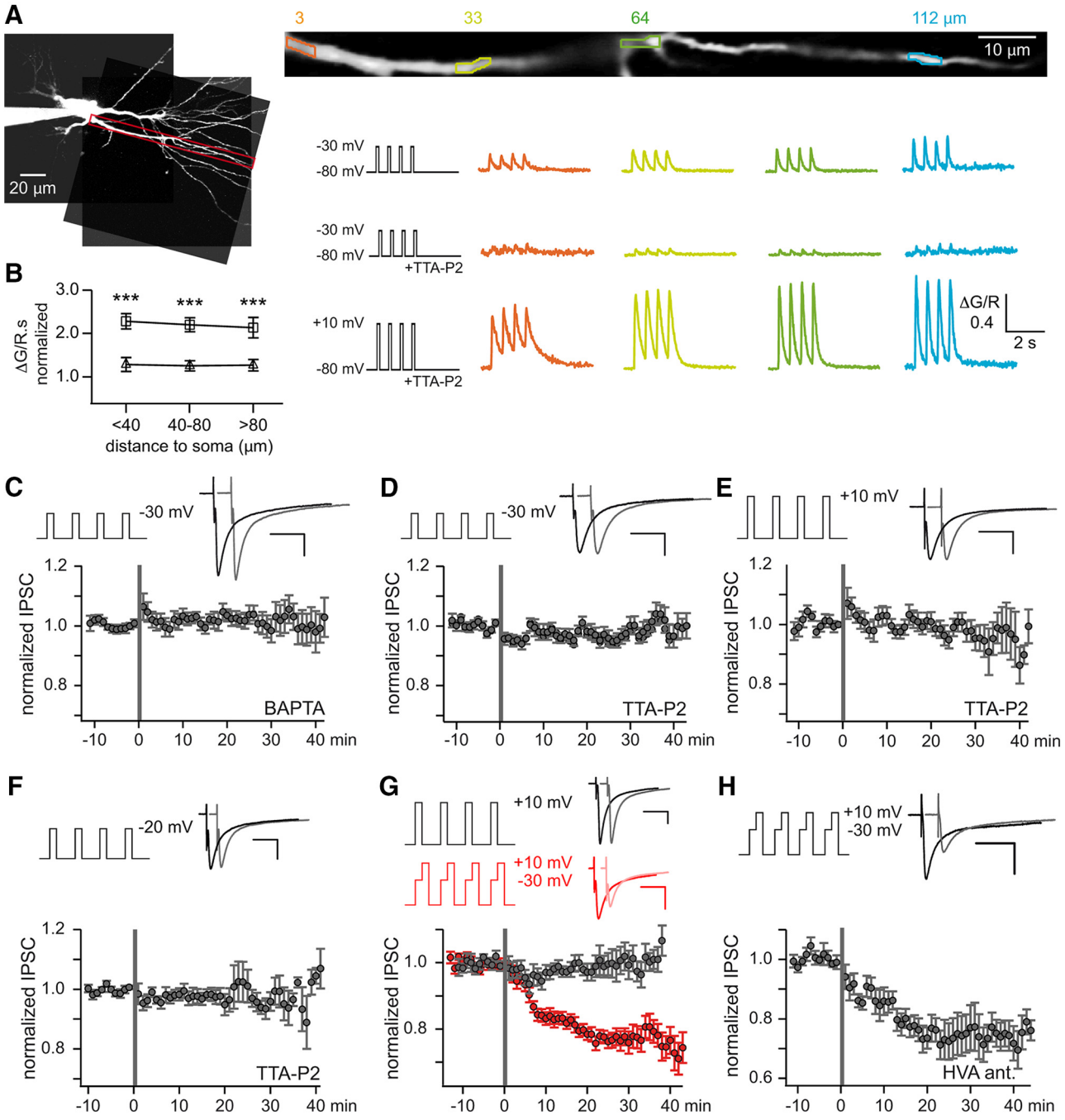

Figure 2. I-LTD induction requires specific activation of T-type calcium currents. ***A***, Dendritic calcium responses evoked by somatic depolarizations in a TC neuron. Left, Stacked two-photon microscopy image of a TC neuron filled with Alexa Fluor 594 and the Ca^{2+}-sensitive dye Fluo-5F. The red box indicates the scanned dendritic part shown at a larger magnification (top line) with the four regions of interest highlighted. Traces below present variations in the fluorescent dye ratio ($\Delta G/R$; see Materials and Methods) indicating Ca^{2+} responses triggered at these locations by successive step depolarizations at 1.6 Hz from −80 to either −30 or +10 mV in control condition or in the presence of the T-channel antagonist, TTA-P2 (3 µM; corresponding protocols are illustrated on the left). Note that TTA-P2 application almost abolished the Ca^{2+} influx evoked in response to depolarizing pulses from −80 to −30 mV while a large Ca^{2+} entry is still observed for step depolarizations to +10 mV that strongly recruit HVA Ca^{2+} channels. ***B***, Average Ca^{2+} responses evoked in the presence of TTA-P2 (3 µM) by somatic step depolarizations from −80 to −20 (triangles) or +10 mV (squares). In each neuron and for the three dendritic locations, Ca^{2+} responses were estimated by integrating over time the fluorescent ratio ($\Delta G/R$.s). The values were then normalized to the ones previously obtained in response to step depolarizations from −80 to −30 mV in the absence of TTA-P2. Note that compared with the responses due to T-channel activation, Ca^{2+} responses evoked through HVA Ca^{2+} channels by depolarization to +10 mV were double in amplitude (***$p < 0.001$) while HVA-mediated Ca^{2+} entry due to step depolarizations to −20 mV were equivalent. ***C–H***, Summary graphs of the I-LTD magnitude under different experimental conditions (same presentation as in Fig. 1*C*). Addition of 10 mM BAPTA in the recording pipette precluded the induction of the I-LTD triggered by paired high-frequency presynaptic stimulations and postsynaptic depolarizations (see protocol in Fig. 1*A*; $n = 11$; ***C***). Similarly, in the presence of 3 µM TTA-P2 in the bath, no I-LTD was induced with paired depolarizations of the TC neurons to −30 mV ($n = 10$; ***D***), +10 mV ($n = 10$; ***E***), or −20 mV ($n = 11$; ***F***). In contrast, in the absence of TTA-P2, two-step depolarizations from −80 to −30 then +10 mV induced the I-LTD ($n = 12$; red symbols and records, ***G***) while IPSCs remained stable when the TC neurons were depolarized directly from −80 to +10 mV ($n = 9$; black symbols and records, ***G***). Finally, two-step depolarizations from −80 to −30 then +10 mV readily induced the I-LTD in the presence of a mixture of HVA Ca^{2+} channel antagonists (1 µM ω-conotoxin GVIA, 20 µM nifedipine, 500 nM SNX-482; HVA ant.; $n = 7$, ***H***). Schemes of the postsynaptic depolarization protocols and IPCSs from representative experiments recorded before and after the induction protocol are shown above each graph. Same calibration applies to all IPSCs (25 ms, 100 pA).

of the inhibitory currents was observed in any of the 11 recorded TC neurons (postprotocol IPSC amplitude: 102 ± 2% of baseline, $p > 0.05$; Fig. 2*C*). In addition, since the −80 to −30 mV depolarization of the TC neurons almost exclusively activated the T-type Ca^{2+} channels, a new series of experiments was performed in the presence of the specific T-current antagonist, TTA-P2 (3 μM), which nearly suppressed all dendritic Ca^{2+} influx (Fig. 2*A*). In line with the previous experiment, no I-LTD was observed in this condition (postprotocol IPSC amplitude: 98 ± 2% of baseline, $n = 10$, $p > 0.05$; Fig. 2*D*) confirming that an increase in intracellular Ca^{2+} in the TC neuron is required for LTD induction.

To determine whether other sources of dendritic Ca^{2+} entry may restore the I-LTD in the presence of the T-channel antagonist, the induction protocol was modified to recruit high voltage-activated (HVA) Ca^{2+} channels during TC neuron depolarization. Although depolarization from −80 to +10 mV induced a robust increase in the dendritic intracellular Ca^{2+} signal up to the more distal monitored compartment (Fig. 2*A*,*B*), IPSC amplitude remained stable throughout the recordings (postprotocol IPSC amplitude: 99 ± 2% of baseline, $n = 10$, $p > 0.05$; Fig. 2*E*). However, since, (1) full recruitment of the HVA channels during the depolarizations to +10 mV induced a two times stronger increase in intradendritic Ca^{2+} concentration than T-channel activation (Fig. 2*B*) and (2) it has been proposed that synaptic LTD may be impeded by especially large Ca^{2+} entry (Artola and Singer, 1993), experiments were repeated while limiting the HVA recruitment by depolarizing the TC neuron to −20 mV only. Even in this condition where the amplitude of the Ca^{2+} influx through HVA channels matched the one previously obtained during T-channel activation (Fig. 2*B*), no I-LTD was observed in any of the 10 recorded TC neurons (postprotocol IPSC amplitude: 98 ± 3% of baseline, $p > 0.05$; Fig. 2*F*). To further assess if I-LTD induced by T-channel activation was not blocked by HVA channel recruitment and the strong associated Ca^{2+} entry, we next performed experiments without T-channel antagonists using depolarizing steps composed of a jump to successively −30 mV and +10 mV to strongly activate T and HVA channels, respectively. As expected, a clear I-LTD was induced when both Ca^{2+} channel families were recruited (postprotocol IPSC amplitude: 77 ± 2% of baseline, $n = 12$, $p < 0.001$; Fig. 2*G*). Finally, in slices prepared from >P15 rats where the NRT-TC synaptic transmission relies on presynaptic Ca^{2+} entries mediated by the P/Q type channels (Iwasaki et al., 2000), the same protocol was applied upon the block of N-, L-, and R-type HVA Ca^{2+} channels by ω-conotoxin GVIA (1 μM), nifedipine (20 μM), and SNX-482 (500 nM), respectively. Normal I-LTD was induced in the presence of this HVA channel antagonist mixture (postprotocol IPSC amplitude: 75 ± 5% of baseline, $n = 8$, $p < 0.01$; Fig. 2*H*), confirming that activation of T-currents is necessary and sufficient to induce the plasticity. Interestingly, however, when the TC neurons were depolarized directly to +10 mV, in absence of both HVA and T-channel antagonists, no I-LTDs were triggered (postprotocol IPSC amplitude: 100 ± 3% of baseline, $n = 9$, $p > 0.05$; Fig. 2*G*). Importantly, although this depolarization to such potentials opens both T and HVA channels, it induced little Ca^{2+} entry through T-channels since the step depolarization is closed to the T-current reversal potential (Perez-Reyes, 2003). These data strongly suggest that I-LTD induction not only specifically requires T-channel activation but also T-type Ca^{2+} currents of significant amplitude.

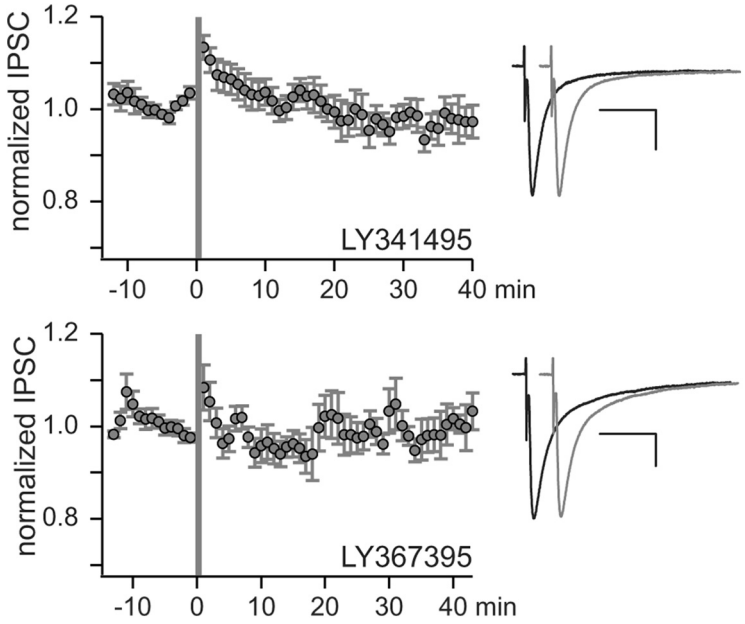

Figure 3. Synaptic activation of mGluRs is necessary for I-LTD induction. Summary graphs of the magnitude of the I-LTD (same presentation as in Fig. 1*C*) showing that addition of the mGluR antagonists, LY-341495 (100 μM, $n = 11$; top graph) or LY-367395 (100 μM, $n = 11$; bottom graph), in the bath precluded the induction of the I-LTD. Same induction protocol as in Figure 1*A*. Same calibration applies to all IPSCs (25 ms, 100 pA).

Activations of both group I metabotropic glutamate receptors and $GABA_A$ receptors are necessary for I-LTD

We next explored which mechanisms triggered by electrical stimulations of the TC neuron afferent fibers were required for I-LTD induction. Since (1) the extracellular stimulation used in our protocol may recruit corticofugal glutamate afferents in addition to the NRT inputs, (2) heterosynaptic plasticity of inhibitory synapses involving mGluRs has been previously reported in other brain areas (Marsicano et al., 2002; Chevaleyre and Castillo, 2003; Azad et al., 2004; Henneberger et al., 2007; Heifets et al., 2008; Adermark and Lovinger, 2009; Jiang et al., 2010), and (3) mGluRs are present on both TC neurons and NRT terminals (Turner and Salt, 2000, 2003), we repeated our experiment in the presence of either the broad-spectrum mGluR antagonist, LY-341495 (100 μM), or the more specific type 1 mGluR antagonist, LY-367385 (100 μM). As shown in Figure 3, both antagonists fully blocked the I-LTD induction (LY-341495: postprotocol IPSC amplitude, 98 ± 3% of baseline, $n = 11$; LY-367385: postprotocol IPSC amplitude, 100 ± 3% of baseline, $n = 11$; $p > 0.05$) demonstrating that the depression of the NRT-TC synapses is controlled by glutamatergic afferences that activate type 1 mGluRs such as those present on TC neurons at corticothalamic synapses (Turner and Salt, 2000).

To test whether this T-channel and mGluR-dependent plasticity affects every GABAergic synapse of the TC neurons or is restricted to the inhibitory pathway activated during the induction protocol, we next simultaneously monitored in the same TC

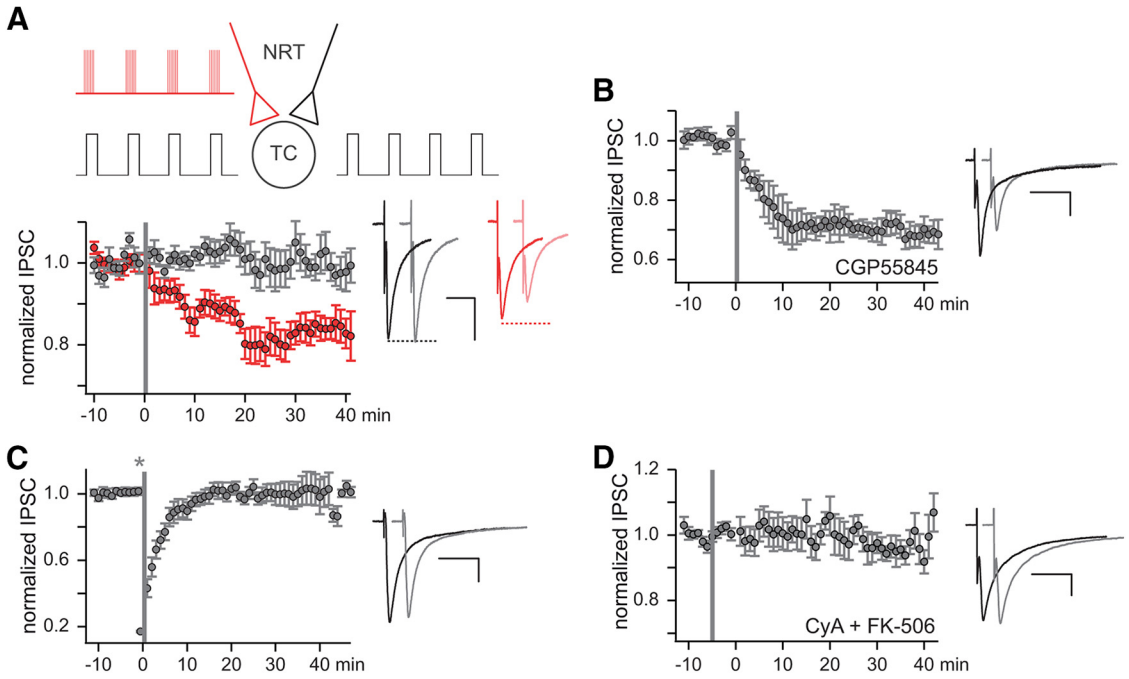

Figure 4. $GABA_A$ receptor activation is required for I-LTD induction. ***A–D***, Summary graphs of the magnitude of the I-LTD (same presentation as in Fig. 1*C*). ***A***, IPSCs evoked in TC neurons in response to the stimulation of two independent inhibitory pathways. Schematic representation of the induction protocol is presented above. Note that one NRT pathway (black) was not stimulated during the induction protocol. For the 11 TC neurons, depression of the IPSCs was only observed for the pathway that underwent the induction protocol including the synaptic stimulation. IPSCs from representative experiments recorded before and after the induction protocol are shown on the right of the graph for the stimulated (red) and nonstimulated (black) pathways. ***B***, Addition of the $GABA_B$ receptor antagonist, CGP-55845 (300 nM, $n = 6$), did not preclude the induction of the I-LTD. Same induction protocol as in Figure 1*A*. ***C***, Puffs of the $GABA_A$ receptor antagonist SR95531 (20 μM, $n = 9$) were applied just before the start of the induction protocol (*). Note that 20 min after this protocol, the IPSCs fully recovered their control amplitude and no I-LTD was triggered. Same induction protocol as in Figure 1*A*. ***D***, Pre-incubation and perfusion with the calcineurin antagonists CyA and FK-506 impeded the I-LTD ($n = 8$). In ***B***, ***C***, and ***D***, IPSCs from representative experiments recorded before (black) and after (gray) the induction protocol are shown to the right of the graph. Same calibration applies to all IPSCs (25 ms, 100 pA).

neuron two GABAergic synapse populations that were stimulated in isolation (see Material and Methods). When high-frequency stimulations were applied to only one of the synapse populations during the induction protocol, I-LTD was induced selectively in this stimulated pathway (postprotocol IPSC amplitude: 80 ± 4% of baseline, $n = 11$, $p < 0.01$) while the amplitude of the IPSCs of the nonstimulated pathway remained stable throughout the recording (postprotocol IPSC amplitude, 100 ± 4% of baseline, $p > 0.05$; Fig. 4*A*). This result shows that, in addition to T-channel and mGluR recruitment, activation of the GABAergic synapses during the induction protocol is required to trigger the LTD.

Presynaptic and postsynaptic $GABA_B$ metabotropic receptors are present at the NRT-TC synapses (Crunelli et al., 1988; Ulrich and Huguenard, 1996; Le Feuvre et al., 1997) and in the ferret thalamus; paired-recordings showed that prolonged burst firing of the perigeniculate neurons activates $GABA_B$-mediated IPSPs in lateral geniculate TC neurons (Kim et al., 1997). As our induction protocol mimics the bursting activity of NRT neurons, we investigated whether these $GABA_B$ receptors contribute to the I-LTD. As shown in Figure 4*B*, in the presence of the specific $GABA_B$ receptor antagonist, CGP-55845 (300 nM), a clear LTD could still be induced (postprotocol IPSC amplitude, 71 ± 3% of baseline, $n = 6$, $p < 0.001$).

We then tested if activation of the $GABA_A$ receptors per se during the induction protocol was required to develop the LTD. To specifically block $GABA_A$ receptors during the induction protocol without compromising our ability to monitor changes in $GABA_A$-mediated IPSCs, we performed, just before the onset of the induction protocol, a 2 s application of the specific $GABA_A$ receptor antagonist, SR95531 (20 μM), which rapidly decreased the IPSC amplitude to 7 ± 1% of the control value ($n = 9$; Fig. 4*C*). Following this short application, IPSCs fully recovered their baseline amplitude 20 min after the induction protocol and no LTD could be observed (postprotocol IPSC amplitude, 102 ± 4% of baseline, $n = 9$, $p > 0.05$; Fig. 4*C*) indicating that $GABA_A$ activation is necessary to trigger the I-LTD.

Requirement of $GABA_A$ receptor activation was previously reported in long-term plasticity mechanisms resulting from a modified chloride reversal potential due to a decrease in the K^+-Cl^- cotransporter, KCC2, activity (Woodin et al., 2003). However, in our recording conditions where TC neurons were dialyzed with a fixed chloride concentration and Cs^+ replaced K^+ as the main intracellular cation, the IPSC amplitude was not changed upon application of 100 μM of the cation/chloride cotransport inhibitor, furosemide (mean IPSC amplitude after furosemide application: 99 ± 2% of baseline, $n = 6$, $p > 0.05$) and I-LTD of the NRT-TC synapses was readily triggered by the induction protocol (postprotocol IPSC amplitude: 79 ± 3% of baseline, $n = 8$, $p < 0.001$; data not shown). Therefore, we concluded that Cl^- cotransporters are not involved in I-LTD of the NRT-TC synapses but that a direct state-dependent modification of the $GABA_A$ receptors may be required. Among the various regulatory intracellular pathways that control $GABA_A$ receptor activity, the Ca^{2+}/calmodulin-dependent phosphatase 2B, calcineurin, has been previously shown to directly interact with the $GABA_A$ receptor γ_2-subunit to mediate LTD at hippocampal inhibitory synapses (Wang et al., 2003). Therefore, we tested whether inhibition of calcineurin by pre-incubation and perfusion of both Cyclosporin A and FK-506 (see Material and Meth-

ods) impeded the I-LTD of the NRT-TC synapses. As shown in Figure 4*D*, no plasticity could be induced in the eight neurons challenged by the induction protocol in this condition (postprotocol IPSC amplitude: 99 ± 4% of baseline, $p > 0.05$).

Discussion

Our results establish that an LTD of the inhibitory synaptic transmission between NRT and TC neurons is triggered by a stimulation paradigm mimicking the thalamic network activity occurring during slow-wave sleep. The mechanism underlying this synaptic plasticity presents unique features, being both heterosynaptic and homosynaptic and requiring calcium entry specifically funneled through T-type Ca^{2+} channels.

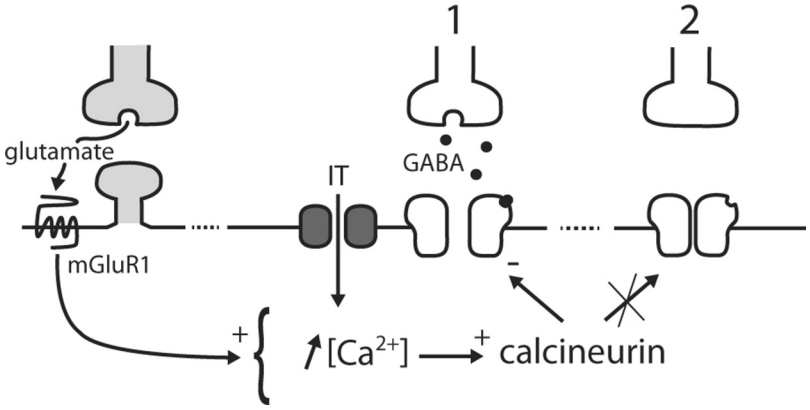

Figure 5. Proposed model of the I-LTD mechanism at NRT-TC synapses. GABA release from NRT terminals (1) activates postsynaptic $GABA_A$ receptors on TC neurons. Concomitantly large influxes of Ca^{2+} through T-type channels result in an increase in calcium concentration leading to the activation of the calcium-sensitive phosphatase calcineurin. Calcineurin will then dephosphorylate the activated $GABA_A$ receptors (1) inducing their long-term desensitization. Conversely the synaptic strength of the nonactivated $GABA_A$ synapses (2) is unchanged. The I-LTD induction is gated by corticothalamic afferents that activate postsynaptic type 1 mGluR.

Heterosynaptic and homosynaptic I-LTD

The block of I-LTD by a specific type 1 mGluR antagonist clearly demonstrates the heterosynaptic nature of the plasticity at the NRT-TC synapses. Involvement of postsynaptic mGluRs in GABAergic synaptic depression has been previously shown in a number of structures (Chevaleyre and Castillo, 2003; Azad et al., 2004; Henneberger et al., 2007; Heifets et al., 2008; Pan et al., 2008; Adermark and Lovinger, 2009; Jiang et al., 2010). In these cases, activation of the postsynaptic mGluRs triggered a retrograde cannabinoid signal resulting in presynaptically induced I-LTDs. In the thalamus, type 1 mGluRs were immunolocalized only postsynaptically on both NRT and TC neurons (Martin et al., 1992; Godwin et al., 1996; Vidnyanszky et al., 1996) and our stimulation protocol may activate type 1 mGluRs on both types of neurons. As we never observed a change in IPSC paired-pulse depression following the I-LTD induction protocols, it is unlikely that the present plasticity involves a decrease in release probability resulting from direct NRT neuron mGluR activation or retrograde signaling due to TC neuron mGluR activation. Since type 1 mGluRs are present postsynaptically to the glutamatergic cortical afferents impinging on TC neurons (Godwin et al., 1996; Vidnyanszky et al., 1996) we propose that, during sleep-like activities, glutamate released by the corticothalamic afferents closely gates the intrathalamic inhibitory plasticity via unknown postsynaptic mechanisms (Fig. 5).

The present I-LTD is also clearly homosynaptic. Indeed, stimulating two independent bundles of NRT GABAergic afferents of a TC neuron showed that I-LTD was only induced in the pathway submitted to high-frequency stimulation during the induction protocol. In addition, a transient block of $GABA_A$ receptors at the time of the induction protocol fully precluded synaptic depression, suggesting that the intracellular mechanisms require Cl^- influx and/or state-dependent modification(s) of the $GABA_A$ receptors. The Ca^{2+}/calmodulin-dependent phosphatase 2B, calcineurin, may participate in the latter mechanism. Indeed, calcineurin that is involved in multiple inhibitory synaptic plasticities (Morishita and Sastry, 1996; Lu et al., 2000; Wang et al., 2003; Dacher et al., 2013) and blocks the present I-LTD directly binds to the $GABA_A$ receptor γ_2-subunits (Wang et al., 2003). γ_2-Subunits mediate receptor synaptic clustering (Essrich et al., 1998) and their viral deletion totally suppress spontaneous and evoked synaptic currents in TC neurons, demonstrating their presence at the NRT-TC synapses (Rovó et al., 2014). Therefore, one can speculate that the TC neuron calcium increase evoked by the induction protocol activates calcineurin resulting in a dephosphorylation of the activated $GABA_A$ receptors, a crucial step in their long-term desensitization (Fig. 5).

Specific activation of T-type calcium channels is required for I-LTD

Buffering postsynaptic calcium blocked the thalamic I-LTD induced by sleep-like activity at the NRT-TC synapses and, although mGluR1 receptors can mobilize calcium from intracellular stores (Ferraguti et al., 2008), depolarization of the TC neurons and recruitment of voltage-dependent Ca^{2+} channels were necessary. Various Ca^{2+} channels were shown to contribute to synaptic plasticity (Cavazzini et al., 2005) and at a given inhibitory synapse, whether LTD or LTP is induced may depend on the ratio of activation of these different calcium channels (Kurotani et al., 2008). Using a combination of pharmacological calcium imaging and electrophysiological approaches, we showed that a significant calcium influx through T-channels was specifically required to induce I-LTD at NRT-TC synapses. The inability of high voltage versus low voltage-activated calcium currents to trigger the synaptic plasticity was not due to differences in amplitude or spatial extent of the rises in intracellular calcium concentration.

In a number of structures, including hippocampus (Oliet et al., 1997), cortex (Birtoli and Ulrich, 2004; Bender et al., 2006; Kampa et al., 2006; Nevian and Sakmann, 2006), cerebellum (Aizenman et al., 1998; Pugh and Raman, 2006; Ly et al., 2013), and thalamus (Astori and Lüthi, 2013; Sieber et al., 2013), T-currents have been involved in synaptic plasticity, although for many years the lack of potent and selective antagonists often precluded the ability to definitely distinguish between R- and T-channel contributions. T-channel activation directly mediates a necessary rise in intracellular Ca^{2+} concentration (Oliet et al., 1997; Bender et al., 2006; Kampa et al., 2006; Nevian and Sakmann, 2006; Pugh and Raman, 2006) and/or generates an initial depolarization that further recruits other Ca^{2+} channels (Aizenman et al., 1998; Birtoli and Ulrich, 2004). However, the requirement of a specific funneling of Ca^{2+} through T-channels as a prerequisite to induce synaptic plasticity was seldom tested and never proved (Nevian

and Sakmann, 2006). Therefore, to the best of our knowledge, our data are the first demonstration of a synaptic plasticity that specifically requires Ca^{2+} entry through T-channels. Since T-channels are mandatory to induce I-LTD at the NRT-TC synapses, one can postulate the existence of preferential link(s) between these channels and other partners of the synaptic plasticity, as local interactions between T-channels and the $GABA_A$ receptors and/or calcineurin. T-channels are known to establish such interactions including direct protein–protein interactions (Anderson et al., 2010, 2013; Engbers et al., 2012), but no data are available concerning a potential colocalization of $GABA_A$ receptors or calcineurin and T-channels.

Physiological relevance of I-LTD in the thalamus

In the thalamic posterior medial nucleus (POM), a long-term potentiation of inhibitory synapses involving a totally different mechanism was recently described (Sieber et al., 2013). This I-LTP was induced by repetitive depolarization of TC neurons from hyperpolarized membrane potentials at very low frequency that evoked low-threshold calcium spikes. The associated Ca^{2+} rise induced the synthesis of nitric oxide, retrogradely activating presynaptic guanylyl cyclase and mediating the presynaptic expression of the I-LTP. In this study, the specific requirement of T-current was not established and L-type Ca^{2+} channel antagonists blocked the I-LTP. However, the dependence of the plasticity on TC neuron bursting, required to depolarize the whole dendritic arbor (Errington et al., 2010), suggests that the I-LTP may occur during sleep when TC neurons discharge in bursts.

Here we demonstrated that I-LTD of the NRT-TC synapses in the VB nucleus required a large Ca^{2+} influx through the T-channels that would also be only expected during slow-wave sleep. At first glance it may be surprising that thalamic sleep rhythms may generate both LTP and LTD of the inhibitory afferents on TC neurons. This discrepancy may be due to the different conditions associated with the recording techniques (current clamp in Sieber et al., 2013 vs voltage clamp in the present study) or the slightly older rats (P17–P21) used by Sieber et al. (2013). However, it must be emphasized that TC neurons of the POM received at least two GABAergic afferents arising not only from the NRT but also from extrareticular sources, the zona incerta and the anterior pretectal nucleus, which display very different anatomical and functional properties (Wanaverbecq et al., 2008). Therefore, it is not clear whether the sleep-related I-LTP affects the reticular or extrareticular GABAergic pathways impinging on POM neurons. In addition, I-LTP was induced with sustained (10 min) bursting activity at very low frequency (0.1 Hz) and was greatly reduced or absent when the bursts occurred at higher frequency (>1 Hz; Sieber et al., 2013). In contrast, we induced I-LTD by evoking short trains of T-currents at 1.6 Hz. Therefore, LTP of inhibitory synapses in POM should develop at early stages of NREM sleep when bursts mainly occur at very low frequency at the TC neuron transitions from DOWN to UP states characteristic of the slow-sleep oscillation. Conversely, LTD at the NRT-TC synapses in VB nucleus should be triggered during a deeper sleep state when the slow oscillation is intermixed with delta-bursting activity at a higher frequency (Crunelli et al., 2006). Accordingly, the direction of the inhibitory plasticity may depend on the precise structure of sleep episodes in a given thalamic area.

Finally, LTP in the POM only required repetitive bursting activity and therefore should develop in all TC neurons and affect every GABAergic synapse. Conversely, the I-LTD required not only T-current generation but also $GABA_A$ and metabotropic glutamate receptor activation (Fig. 5). Therefore, I-LTD is a more restricted process that specifically affects activated GABAergic synapses in a subset of TC neurons submitted to strong activation of their corticothalamic inputs, and hence may be involved in the precise functional reshaping of the sensory information pathway during sleep. Indeed, since NRT neurons are involved in sensory processing (Yu et al., 2009; Halassa et al., 2014) and selective attention (McAlonan et al., 2008), cortically controlled depression of the NRT-TC synapse should markedly affect sensory information transfer to the cortex. In addition, in the context of sleep-associated cognitive functions, plasticities of NRT-TC synapses affect the basic network of spindle generation (Bal et al., 1995) with potential drastic consequences on sleep-dependent memory consolidation (Diekelmann and Born, 2010).

References

Adermark L, Lovinger DM (2009) Frequency-dependent inversion of net striatal output by endocannabinoid-dependent plasticity at different synaptic inputs. J Neurosci 29:1375–1380. CrossRef Medline

Aizenman CD, Manis PB, Linden DJ (1998) Polarity of long-term synaptic gain change is related to postsynaptic spike firing at a cerebellar inhibitory synapse. Neuron 21:827–835. CrossRef Medline

Amzica F, Nuñez A, Steriade M (1992) Delta frequency (1–4 Hz) oscillations of perigeniculate thalamic neurons and their modulation by light. Neuroscience 51:285–294. CrossRef Medline

Anderson D, Mehaffey WH, Iftinca M, Rehak R, Engbers JD, Hameed S, Zamponi GW, Turner RW (2010) Regulation of neuronal activity by Cav3-Kv4 channel signaling complexes. Nat Neurosci 13:333–337. CrossRef Medline

Anderson D, Engbers JD, Heath NC, Bartoletti TM, Mehaffey WH, Zamponi GW, Turner RW (2013) The Cav3-Kv4 complex acts as a calcium sensor to maintain inhibitory charge transfer during extracellular calcium fluctuations. J Neurosci 33:7811–7824. CrossRef Medline

Artola A, Singer W (1993) Long-term depression of excitatory synaptic transmission and its relationship to long-term potentiation. Trends Neurosci 16:480–487. CrossRef Medline

Astori S, Lüthi A (2013) Synaptic plasticity at intrathalamic connections via CaV3.3 T-type Ca2+ channels and GluN2B-containing NMDA receptors. J Neurosci 33:624–630. CrossRef Medline

Azad SC, Monory K, Marsicano G, Cravatt BF, Lutz B, Zieglgänsberger W, Rammes G (2004) Circuitry for associative plasticity in the amygdala involves endocannabinoid signaling. J Neurosci 24:9953–9961. CrossRef Medline

Bal T, von Krosigk M, McCormick DA (1995) Synaptic and membrane mechanisms underlying synchronized oscillations in the ferret lateral geniculate nucleus in vitro. J Physiol 483:641–663. Medline

Bender VA, Bender KJ, Brasier DJ, Feldman DE (2006) Two coincidence detectors for spike timing-dependent plasticity in somatosensory cortex. J Neurosci 26:4166–4177. CrossRef Medline

Birtoli B, Ulrich D (2004) Firing mode-dependent synaptic plasticity in rat neocortical pyramidal neurons. J Neurosci 24:4935–4940. CrossRef Medline

Castro-Alamancos MA, Calcagnotto ME (1999) Presynaptic long-term potentiation in corticothalamic synapses. J Neurosci 19:9090–9097. Medline

Cavazzini M, Bliss T, Emptage N (2005) Ca2+ and synaptic plasticity. Cell Calcium 38:355–367. CrossRef Medline

Chausson P, Leresche N, Lambert RC (2013) Dynamics of intrinsic dendritic calcium signaling during tonic firing of thalamic reticular neurons. PLoS One 8:e72275. CrossRef Medline

Chevaleyre V, Castillo PE (2003) Heterosynaptic LTD of hippocampal GABAergic synapses: a novel role of endocannabinoids in regulating excitability. Neuron 38:461–472. CrossRef Medline

Citri A, Malenka RC (2008) Synaptic plasticity: multiple forms, functions, and mechanisms. Neuropsychopharmacology 33:18–41. CrossRef Medline

Contreras D, Steriade M (1997) State-dependent fluctuations of low-frequency rhythms in corticothalamic networks. Neuroscience 76:25–38. CrossRef Medline

Crandall SR, Govindaiah G, Cox CL (2010) Low-threshold Ca2+ current

amplifies distal dendritic signaling in thalamic reticular neurons. J Neurosci 30:15419–15429. CrossRef Medline

Crick F (1984) Function of the thalamic reticular complex: the searchlight hypothesis. Proc Natl Acad Sci U S A 81:4586–4590. CrossRef Medline

Crunelli V, Leresche N (2002) Childhood absence epilepsy: genes, channels, neurons and networks. Nat Rev Neurosci 3:371–382. CrossRef Medline

Crunelli V, Haby M, Jassik-Gerschenfeld D, Leresche N, Pirchio M (1988) Cl- and K+-dependent inhibitory postsynaptic potentials evoked by interneurones of the rat lateral geniculate nucleus. J Physiol 399:153–176. Medline

Crunelli V, Cope DW, Hughes SW (2006) Thalamic T-type Ca2+ channels and NREM sleep. Cell Calcium 40:175–190. CrossRef Medline

Dacher M, Gouty S, Dash S, Cox BM, Nugent FS (2013) A-kinase anchoring protein-calcineurin signaling in long-term depression of GABAergic synapses. J Neurosci 33:2650–2660. CrossRef Medline

Diekelmann S, Born J (2010) The memory function of sleep. Nat Rev Neurosci 11:114–126. Medline

Domich L, Oakson G, Steriade M (1986) Thalamic burst patterns in the naturally sleeping cat: a comparison between cortically projecting and reticularis neurones. J Physiol 379:429–449. Medline

Engbers JD, Anderson D, Asmara H, Rehak R, Mehaffey WH, Hameed S, McKay BE, Kruskic M, Zamponi GW, Turner RW (2012) Intermediate conductance calcium-activated potassium channels modulate summation of parallel fiber input in cerebellar Purkinje cells. Proc Natl Acad Sci U S A 109:2601–2606. CrossRef Medline

Errington AC, Renger JJ, Uebele VN, Crunelli V (2010) State-dependent firing determines intrinsic dendritic Ca2+ signaling in thalamocortical neurons. J Neurosci 30:14843–14853. CrossRef Medline

Essrich C, Lorez M, Benson JA, Fritschy JM, Lüscher B (1998) Postsynaptic clustering of major GABAA receptor subtypes requires the gamma 2 subunit and gephyrin. Nat Neurosci 1:563–571. CrossRef Medline

Ferraguti F, Crepaldi L, Nicoletti F (2008) Metabotropic glutamate 1 receptor: current concepts and perspectives. Pharmacol Rev 60:536–581. CrossRef Medline

Godwin DW, Van Horn SC, Eriir A, Sesma M, Romano C, Sherman SM (1996) Ultrastructural localization suggests that retinal and cortical inputs access different metabotropic glutamate receptors in the lateral geniculate nucleus. J Neurosci 16:8181–8192. Medline

Halassa MM, Chen Z, Wimmer RD, Brunetti PM, Zhao S, Zikopoulos B, Wang F, Brown EN, Wilson MA (2014) State-dependent architecture of thalamic reticular subnetworks. Cell 158:808–821. CrossRef Medline

Heifets BD, Chevaleyre V, Castillo PE (2008) Interneuron activity controls endocannabinoid-mediated presynaptic plasticity through calcineurin. Proc Natl Acad Sci U S A 105:10250–10255. CrossRef Medline

Henneberger C, Redman SJ, Grantyn R (2007) Cortical efferent control of subcortical sensory neurons by synaptic disinhibition. Cereb Cortex 17:2039–2049. CrossRef Medline

Higley MJ, Contreras D (2007) Cellular mechanisms of suppressive interactions between somatosensory responses in vivo. J Neurophysiol 97:647–658. CrossRef Medline

Iwasaki S, Momiyama A, Uchitel OD, Takahashi T (2000) Developmental changes in calcium channel types mediating central synaptic transmission. J Neurosci 20:59–65. Medline

Jiang B, Huang S, de Pasquale R, Millman D, Song L, Lee HK, Tsumoto T, Kirkwood A (2010) The maturation of GABAergic transmission in visual cortex requires endocannabinoid-mediated LTD of inhibitory inputs during a critical period. Neuron 66:248–259. CrossRef Medline

Kampa BM, Letzkus JJ, Stuart GJ (2006) Cortical feed-forward networks for binding different streams of sensory information. Nat Neurosci 9:1472–1473. CrossRef Medline

Kim U, Sanchez-Vives MV, McCormick DA (1997) Functional dynamics of GABAergic inhibition in the thalamus. Science 278:130–134. CrossRef Medline

Kurotani T, Yamada K, Yoshimura Y, Crair MC, Komatsu Y (2008) State-dependent bidirectional modification of somatic inhibition in neocortical pyramidal cells. Neuron 57:905–916. CrossRef Medline

Le Feuvre Y, Fricker D, Leresche N (1997) GABAA receptor-mediated IPSCs in rat thalamic sensory nuclei: patterns of discharge and tonic modulation by GABAB autoreceptors. J Physiol 502:91–104. CrossRef Medline

Leresche N, Lambert RC, Errington AC, Crunelli V (2012) From sleep spindles of natural sleep to spike and wave discharges of typical absence seizures: is the hypothesis still valid? Pflugers Arch 463:201–212. CrossRef Medline

Lu YM, Mansuy IM, Kandel ER, Roder J (2000) Calcineurin-mediated LTD of GABAergic inhibition underlies the increased excitability of CA1 neurons associated with LTP. Neuron 26:197–205. CrossRef Medline

Ly R, Bouvier G, Schonewille M, Arabo A, Rondi-Reig L, Léna C, Casado M, De Zeeuw CI, Feltz A (2013) T-type channel blockade impairs long-term potentiation at the parallel fiber-Purkinje cell synapse and cerebellar learning. Proc Natl Acad Sci U S A 110:20302–20307. CrossRef Medline

Marsicano G, Wotjak CT, Azad SC, Bisogno T, Rammes G, Cascio MG, Hermann H, Tang J, Hofmann C, Zieglgänsberger W, Di Marzo V, Lutz B (2002) The endogenous cannabinoid system controls extinction of aversive memories. Nature 418:530–534. CrossRef Medline

Martin LJ, Blackstone CD, Huganir RL, Price DL (1992) Cellular localization of a metabotropic glutamate receptor in rat brain. Neuron 9:259–270. CrossRef Medline

McAlonan K, Cavanaugh J, Wurtz RH (2006) Attentional modulation of thalamic reticular neurons. J Neurosci 26:4444–4450. CrossRef Medline

McAlonan K, Cavanaugh J, Wurtz RH (2008) Guarding the gateway to cortex with attention in visual thalamus. Nature 456:391–394. CrossRef Medline

Morishita W, Sastry BR (1996) Postsynaptic mechanisms underlying long-term depression of GABAergic transmission in neurons of the deep cerebellar nuclei. J Neurophysiol 76:59–68. Medline

Nevian T, Sakmann B (2006) Spine Ca2+ signaling in spike-timing-dependent plasticity. J Neurosci 26:11001–11013. CrossRef Medline

Nguyen QT, Tsai PS, Kleinfeld D (2006) MPScope: a versatile software suite for multiphoton microscopy. J Neurosci Methods 156:351–359. CrossRef Medline

Oliet SH, Malenka RC, Nicoll RA (1997) Two distinct forms of long-term depression coexist in CA1 hippocampal pyramidal cells. Neuron 18:969–982. CrossRef Medline

Pan B, Hillard CJ, Liu QS (2008) D2 dopamine receptor activation facilitates endocannabinoid-mediated long-term synaptic depression of GABAergic synaptic transmission in midbrain dopamine neurons via cAMP-protein kinase A signaling. J Neurosci 28:14018–14030. CrossRef Medline

Perez-Reyes E (2003) Molecular physiology of low-voltage-activated t-type calcium channels. Physiol Rev 83:117–161. Medline

Pugh JR, Raman IM (2006) Potentiation of mossy fiber EPSCs in the cerebellar nuclei by NMDA receptor activation followed by postinhibitory rebound current. Neuron 51:113–123. CrossRef Medline

Rovó Z, Mátyás F, Barthó P, Slézia A, Lecci S, Pellegrini C, Astori S, Dávid C, Hangya B, Lüthi A, Acsády L (2014) Phasic, nonsynaptic GABA-A receptor-mediated inhibition entrains thalamocortical oscillations. J Neurosci 34:7137–7147. CrossRef Medline

Sherman SM, Guillery RW (1996) Functional organization of thalamocortical relays. J Neurophysiol 76:1367–1395. Medline

Sieber AR, Min R, Nevian T (2013) Non-Hebbian long-term potentiation of inhibitory synapses in the thalamus. J Neurosci 33:15675–15685. CrossRef Medline

Steriade M, McCormick DA, Sejnowski TJ (1993) Thalamocortical oscillations in the sleeping and aroused brain. Science 262:679–685. CrossRef Medline

Tononi G, Cirelli C (2014) Sleep and the price of plasticity: from synaptic and cellular homeostasis to memory consolidation and integration. Neuron 81:12–34. CrossRef Medline

Turner JP, Salt TE (2000) Synaptic activation of the group I metabotropic glutamate receptor mGlu1 on the thalamocortical neurons of the rat dorsal lateral geniculate nucleus in vitro. Neuroscience 100:493–505. CrossRef Medline

Turner JP, Salt TE (2003) Group II and III metabotropic glutamate receptors and the control of the nucleus reticularis thalami input to rat thalamocortical neurones in vitro. Neuroscience 122:459–469. CrossRef Medline

Ulrich D, Huguenard JR (1996) GABAB receptor-mediated responses in

GABAergic projection neurones of rat nucleus reticularis thalami in vitro. J Physiol 493:845–854. Medline

Vidnyanszky Z, Gorcs TJ, Negyessy L, Borostyankio Z, Knopfel T, Hamori J (1996) Immunocytochemical visualization of the mGluR1a metabotropic glutamate receptor at synapses of corticothalamic terminals originating from area 17 of the rat. Eur J Neurosci 8:1061–1071. CrossRef Medline

Wanaverbecq N, Bodor AL, Bokor H, Slezia A, Lüthi A, Acsády L (2008) Contrasting the functional properties of GABAergic axon terminals with single and multiple synapses in the thalamus. J Neurosci 28:11848–11861. CrossRef Medline

Wang J, Liu S, Haditsch U, Tu W, Cochrane K, Ahmadian G, Tran L, Paw J, Wang Y, Mansuy I, Salter MM, Lu YM (2003) Interaction of calcineurin and type-A GABA receptor gamma 2 subunits produces long-term depression at CA1 inhibitory synapses. J Neurosci 23:826–836. Medline

Weese GD, Phillips JM, Brown VJ (1999) Attentional orienting is impaired by unilateral lesions of the thalamic reticular nucleus in the rat. J Neurosci 19:10135–10139. Medline

Woodin MA, Ganguly K, Poo MM (2003) Coincident presynaptic and postsynaptic activity modifies GABAergic synapses by postsynaptic changes in Cl- transporter activity. Neuron 39:807–820. CrossRef Medline

Yu XJ, Xu XX, He S, He J (2009) Change detection by thalamic reticular neurons. Nat Neurosci 12:1165–1170. CrossRef Medline